

Remarks on the KARMEN anomaly

V. Barger^a, R.J.N. Phillips^b and S. Sarkar^c

^a*Physics Department, University of Wisconsin, Madison, WI 53706, USA*

^b*Rutherford Appleton Laboratory, Chilton, Didcot, Oxon OX11 0QX, UK*

^c*Theoretical Physics, University of Oxford, 1 Keble Road, Oxford OX1 3NP, UK*

Abstract

A recently reported anomaly in the time structure of signals in the KARMEN neutrino detector suggests the decay of a new particle x , produced in $\pi^+ \rightarrow \mu^+ x$ with mass $m_x = 33.9$ MeV. We discuss the constraints and difficulties in interpreting x as a neutrino. We show that a mainly-sterile neutrino scenario is compatible with all laboratory constraints, within narrow limits on the mixing parameters, although there are problems with astrophysical and cosmological constraints. This scenario predicts that appreciable numbers of other x -decay events with different origins and time structures should also be observable in the KARMEN detector. Such x -decay events should also be found in the LSND experiment and may be relevant to the search for $\bar{\nu}_\mu \rightarrow \bar{\nu}_e$ oscillations.

(Published in *Phys. Lett. B352 (1995) 365*; erratum added June 1995)

The KARMEN collaboration, which studies the interactions of neutrinos from the stopped π^+ decay chain at RAL, has recently reported an anomaly [1] in the time-dependence of their signals. This anomaly suggests the production of a new weakly-interacting neutral particle (call it x) in the initial π^+ decays, which travels with well determined velocity $\beta_x = v_x/c \simeq 1/60$ and decays in the detector after a mean flight path of 17.5 m. The distinctive feature of the x -events is their timing, apparently at a well determined interval $3.6\mu\text{s}$ after the arrival and prompt decay of the pion pulse (which determines β_x); however, the visible energy in the detector scintillator shows no anomaly, so x decays apparently deposit visible energy similar to typical neutrino interactions. The present note briefly discusses the interpretation of x as a massive neutrino. We show that a mainly-sterile neutrino scenario is compatible with all laboratory constraints, for either Dirac or Majorana options, within rather narrow bounds on the mixing parameters. There are some problems with astrophysical and cosmological constraints, but it is interesting nevertheless to explore the further implications for laboratory experiments which can test this interpretation directly. This scenario predicts that appreciable numbers of other x -decay events with different origins and time structures should also be observable in the KARMEN detector. Such x -decay events should also be found in the LSND experiment at LAMPF [2] and may be relevant to the ongoing search for $\bar{\nu}_\mu \rightarrow \bar{\nu}_e$ oscillations [3].

If we postulate no other new particles below the pion mass, then the precise time structure [1] requires x production to go via one of the two-body modes $\pi^+ \rightarrow \mu^+ x$ or $\pi^+ \rightarrow e^+ x$. However the latter implies mass $m_x = 137.2$ MeV (determined from β_x) and hence anomalously large visible x -decay energy, with mean value $\langle T_{\text{vis}} \rangle \simeq 51$ MeV for $x \rightarrow \mu e \nu \rightarrow e e \nu \nu$ or $\langle T_{\text{vis}} \rangle \simeq 88$ MeV for $x \rightarrow e e \nu$, compared to neutrino interactions that typically give $T_{\text{vis}} \sim 11 - 35$ MeV [1]. We must therefore presume that x is produced via $\pi^+ \rightarrow \mu^+ x$, with $m_x = 33.9$ MeV determined from β_x . Assuming no new weak interactions, the standard decay mode is $x \rightarrow e^- e^+ \nu_e$; note that flavour-changing neutral current (FCNC) processes $x \rightarrow \nu \nu \nu$ and $x \rightarrow \nu \gamma$ are highly suppressed for a standard isodoublet neutrino (we consider the isosinglet case later) [4,5].

The neutrino charged-current eigenstates $\nu_{\alpha L}$ ($\alpha = e, \mu, \tau$) which appear in the weak interaction coupled via W to e, μ, τ , may be written as coherent superpositions of mass

eigenstates ν_{iL} ($i = 1, 2, \dots, x$) using the usual mixing matrix $U_{\alpha i}$;

$$\nu_{\alpha L} = \sum_i U_{\alpha i} \nu_{iL} . \quad (1)$$

(In general U is a $n \times n$ matrix, with α running over all $SU(2)_L$ multiplet assignments and i running over all masses). Then the x production and decay processes are scaled by factors $|U_{\mu x}|^2$ and $|U_{ex}|^2$, respectively:

$$\frac{\Gamma(\pi \rightarrow \mu x)}{\Gamma(\pi \rightarrow \mu \nu)} = \frac{|U_{\mu x}|^2 [m_\pi^2 (m_\mu^2 + m_x^2) - (m_\mu^2 - m_x^2)^2] \lambda^{\frac{1}{2}}(m_\pi^2, m_\mu^2, m_x^2)}{m_\mu^2 (m_\pi^2 - m_\mu^2)^2}, \quad (2)$$

$$\frac{\Gamma(x \rightarrow e^+ e^- \nu_e)}{\Gamma(\mu \rightarrow \nu_\mu \bar{\nu}_e e)} = \frac{|U_{ex}|^2 m_x^5}{m_\mu^5} [\text{Dirac}] , \quad \frac{2|U_{ex}|^2 m_x^5}{m_\mu^5} [\text{Majorana}] , \quad (3)$$

where $\lambda(a, b, c) = a^2 + b^2 + c^2 - 2ab - 2bc - 2ca$ and we neglect m_e^2/m_x^2 ; we recall that Majorana neutrinos decay twice as fast as Dirac neutrinos with the same coupling, because their right chiral components are not inert. Hence the production branching fraction and mean decay lifetime are simply given by

$$B(\pi \rightarrow \mu x) = 0.0285 |U_{\mu x}|^2, \quad (4)$$

$$\tau(x \rightarrow ee\nu) = 645 |U_{ex}|^{-2} \mu\text{s} [\text{Dirac}] , \quad \tau(x \rightarrow ee\nu) = 323 |U_{ex}|^{-2} \mu\text{s} [\text{Majorana}] . \quad (5)$$

The correlation between branching fraction and lifetime, needed to explain the KARMEN anomaly, was shown as a curve in the (τ, B) plane in Ref. [1]. We reproduce this as the solid curve in Fig.1, extrapolating along the dashed curve with fixed B/τ , and showing also the scales of $|U_{ex}|^2$ and $|U_{\mu x}|^2$ implied by Eqs.(4)-(5) along the upper and right-hand edges of the diagram (the Dirac option is illustrated for $|U_{ex}|^2$). The regions with $|U_{\alpha x}|^2 > 1$ have no physical meaning in our scenario.

Direct experimental constraints on the mixing elements $|U_{\alpha i}|$ are summarized in Ref. [6]; they generally depend on mass and the constraints we quote below are all for $m_x = 33.9$ MeV. Absence of a correction to the ρ parameter of the e spectrum in $\mu \rightarrow e\nu\nu$ decay gives [7]

$$|U_{ex}|^2 + |U_{\mu x}|^2 < 2 \times 10^{-3}. \quad (6)$$

Absence of decay events in neutrino beams gives [8,9,10]

$$|U_{ex}| |U_{\mu x}| < 1.5 \times 10^{-5}. \quad (7)$$

Absence of anomalous contributions to $\pi \rightarrow e\nu$ gives [11]

$$|U_{ex}|^2 < 0.85 \times 10^{-6}. \quad (8)$$

Limits from neutrinoless $\beta\beta$ -decay searches [12] on the effective ν_e Majorana mass $\langle m_{\nu e} \rangle = |\sum_j \eta_j m_j U_{ej}^2|$, where $\eta_j = \pm$ is the CP signature of Majorana neutrino ν_j , would require (see also Ref. [13])

$$|U_{ex}|^2 \lesssim 6 \times 10^{-8} \quad [\text{Majorana}] , \quad (9)$$

where we have conservatively taken $\langle m_{\nu e} \rangle < 2$ eV [12]. This bound would apply if x were a Majorana state and there were no substantial cancellations in the sum but not if x were a Dirac neutrino or part of a quasi-Dirac pair (with opposite CP signatures). Other direct laboratory constraints are weaker than these [6]. Studies of short muon tracks in $\pi \rightarrow \mu \rightarrow e$ events, from pions stopping in emulsion, would give stringent constraints on $|U_{\mu x}|$ for $m_x < 33$ MeV [7]; but for the present value $m_x = 33.9$ MeV, the muon kinetic energy is only 1.5 keV giving an unobservable track length less than 1 micron, so no constraint can be derived on this basis. The x mass and mixing predict a contribution to the $\mu \rightarrow e\gamma$ branching fraction [14]

$$B(\mu \rightarrow e\gamma) = 3\alpha m_x^2 / (32\pi M_W^2) |U_{ex}^* U_{\mu x}|^2 \simeq 2.5 \times 10^{-23}, \quad (10)$$

a factor $\sim 2 \times 10^{12}$ below the experimental upper limit [6]. The constraints of Eqs.(6)-(8) are shown on Fig.1; they leave a range of “solutions” to the KARMEN anomaly, based on $x \rightarrow e^- e^+ \nu$ decay, described by

$$|U_{ex}| |U_{\mu x}| \simeq 0.8 \times 10^{-6} \quad [\text{Dirac}] , \quad 0.6 \times 10^{-6} \quad [\text{Majorana}] , \quad (11)$$

$$|U_{\mu x}| \lesssim 4.5 \times 10^{-2}, \quad (12)$$

$$|U_{ex}| \lesssim 10^{-3} \quad [\text{Dirac}] , \quad 2.5 \times 10^{-4} \quad [\text{Majorana}] . \quad (13)$$

There are also constraints on the mass and identification of x . The ARGUS bound $m(\nu_\tau) < 31$ MeV [15], the CLEO bound $m(\nu_\tau) < 32.6$ MeV [16] and the recent ALEPH bound $m(\nu_\tau) < 24$ MeV [17] (all at 95% C.L.), exclude x from being the major component of ν_τ . Since LEP experiments measure $N_\nu = 2.988 \pm 0.023$ [18] light neutrino species (weighted by their isodoublet mixing factors), the chiral component x_L participating in standard weak interactions must then be dominantly isosinglet, i.e. sterile.

An isodoublet interpretation of x is also excluded by cosmological and astrophysical arguments concerning unstable neutrinos in the mass and lifetime range of interest [19]. If x has standard weak interactions, its cosmological relic abundance would be sufficiently

high that its decay products would have distorted the spectrum of the 2.73 K blackbody radiation background unless its lifetime were less than $\sim 10^5$ s [20,21]. This requires $|U_{ex}|^2 \gtrsim 10^{-8}$ (for $m_x = 33.9$ MeV) and removes part of the solution range in Eq.(13). At such early times the background photons are energetic enough to be Compton scattered by the e^+e^- pairs from x decay to energies above the ^2H photofission threshold and may thus undo nucleosynthesis [21]. Taking into account the energy degradation due to $\gamma - \gamma$ scattering [22] this sets a lifetime bound of $\lesssim 2 \times 10^3$ s [23] corresponding to $|U_{ex}|^2 \gtrsim 5 \times 10^{-7}$, which leaves only a tiny region of the remaining solution range. (Further constraints on isodoublets from consideration of the entropy production by the decaying particle are rather sensitive to the adopted upper limit to the primordial ^4He abundance [24].) This loophole is closed by consideration of the production and decays of massive neutrinos in Supernova 1987A. For example the process $x \rightarrow \nu_e e^+ e^- \gamma$ operates at a rate $\alpha/2\pi$ relative to the decay $x \rightarrow \nu_e e^+ e^-$ and would have generated a γ ray burst which was not observed by the SMM satellite [25]. When combined with other arguments relating to energy deposition inside the supernova [26], as well as experimental bounds on fast ν_τ decays [8,9], this rules out *all* lifetimes shorter than $\sim 10^8$ s [27], forbidding the entire solution range for doublet neutrinos.

In order to evade the above bounds, it may appear adequate to require x to be mainly sterile since its direct production, both in supernovae and in the early universe, is then suppressed. However, sterile neutrinos can also be produced through their mixing with doublet neutrinos, modulated by matter effects. During the collapse phase of a supernova, resonant $\nu_e \rightarrow x$ conversions may cause rapid deleptonisation of the core which would probably prevent the supernova explosion [28]; however this does not happen for $\Delta m^2 \gtrsim 10^8$ eV² so will not apply to the x particle. Secondly the energy loss due to emission of sterile neutrinos during the cooling phase would have excessively shortened the $\bar{\nu}_e$ burst from SN 1987A for a mixing in the range $|U_{ex}|^2 \sim 10^{-9} - 10^{-2}$ [29]; this argument applies to a neutrino with mass up to $\sim 50 - 100$ MeV [30] (see also Ref. [13]) and will rule out the allowed region for x . Most crucially, the absence of a γ ray burst from SN 1987A would, as in the case of doublet neutrinos discussed above, rule out radiative decays [30] with lifetimes in the range $\sim 10^1 - 10^8$ s, taking into account the enhancement of radiative decays for a singlet neutrino (see below). The production of sterile neutrinos through neutrino oscillations in the early universe [31] also presents

a problem since x particles can be brought into thermal equilibrium at temperatures exceeding a few GeV. Although the x relic abundance is thus substantially diluted by the entropy release during the subsequent quark-hadron phase transition, x decays with a lifetime $\gtrsim 0.1$ s will have an adverse effect on primordial nucleosynthesis [32] (see also Ref. [13]). Thus the interpretation of the KARMEN anomaly as a singlet neutrino is severely challenged by astrophysical and cosmological arguments, although there may be a loophole for fast decays with lifetime $\ll 0.1$ s which occur in the supernova core and, in the early universe, before nucleosynthesis. Therefore we proceed to examine the implications of this hypothesis for laboratory experiments which can test it definitively.

Identifying x as mainly sterile has several distinct repercussions for the x -decay modes, since GIM cancellations no longer suppress FCNC:

(i) The $x \rightarrow \nu\nu\nu$ invisible modes are now appreciable; we obtain

$$\Gamma(x \rightarrow \nu\nu\nu)/\Gamma(x \rightarrow e^-e^+\nu_e) = [|U_{ex}|^2 + |U_{\mu x}|^2 + |U_{\tau x}|^2] / |U_{ex}|^2, \quad (14)$$

assuming that just one singlet neutrino flavour takes part and the other 3 neutrinos are much lighter than x ; thus the invisible branching fraction is never less than 50%. But our determination of $|U_{ex}|^2$ from the KARMEN B/τ plot is preserved, because the latter is determined by the visible decays only: $\tau = \Gamma(x \rightarrow \text{vis})^{-1}$. Adding invisible decay modes increases the total x -width and hence the total number of decays in a given detector, but the visible fraction decreases by the same factor and the number of visible decays remains unchanged (so long as the distance to the detector remains much less than the mean decay length, which is the case here).

(ii) Radiative decays $x \rightarrow \nu\gamma$, going via loop diagrams, also escape GIM suppression for mainly-singlet x ; we obtain [4,5]

$$\Gamma(x \rightarrow \nu\gamma)/\Gamma(x \rightarrow \nu\nu\nu) = \frac{27\alpha}{8\pi} = \frac{1}{128}, \quad (15)$$

assuming one singlet and summing 3 light final flavours as before. Radiative decays are thus between 0.4% and 0.8% of total decays, but can dominate visible decays as follows:

$$|U_{\mu x}|^2 + |U_{\tau x}|^2 > 127 |U_{ex}|^2, \quad x \rightarrow \nu\gamma \text{ dominates}; \quad (16)$$

$$|U_{\mu x}|^2 + |U_{\tau x}|^2 < 127 |U_{ex}|^2, \quad x \rightarrow e^-e^+\nu \text{ dominates}. \quad (17)$$

(iii) When $x \rightarrow \nu\gamma$ modes start to dominate over $x \rightarrow e^-e^+\nu$ in the visible decays, we can no longer compensate an increase in x -production (increase in $|U_{\mu x}|^2$) by a decrease

in $|U_{ex}|^2$, so we have to add Eq.(17) to the solution constraints for a sterile neutrino. This leaves a reasonable range for sterile Dirac but only a small region for sterile Majorana solutions in Fig.1.

(iv) A new class of solution is possible, in which $x \rightarrow \nu\gamma$ dominates the visible decays, in contrast to the solutions displayed in Fig.1 where $x \rightarrow e^-e^+\nu$ dominates. These solutions have $B \times \Gamma(x \rightarrow \text{vis}) \simeq 3 \times 10^{-17} \mu\text{s}^{-1}$ with B determined by Eq.(4) as before, but $|U_{ex}|^2$ now contributes negligibly to the decay and we have $\Gamma(x \rightarrow \text{vis}) = 1.2 \times 10^{-5}(|U_{\mu x}|^2 + |U_{\tau x}|^2) \mu\text{s}^{-1}$ for Dirac x (double this for Majorana x). Hence these solutions are characterized by

$$|U_{\mu x}|^2(|U_{\mu x}|^2 + |U_{\tau x}|^2) \simeq 0.8 \times 10^{-10} \text{ [Dirac]}, \quad 0.4 \times 10^{-10} \text{ [Majorana]}, \quad (18)$$

which automatically satisfies the requirement $|U_{\mu x}|^2 < 2 \times 10^{-3}$ from Eq.(6). They are also constrained by the preliminary bound on $\nu_\tau \rightarrow \nu_i\gamma$ decays [33] from the BEBC-WA66 beam dump experiment [9], which here translates into

$$|U_{\tau x}|^2(|U_{\mu x}|^2 + |U_{\tau x}|^2) \lesssim 0.016 \text{ [Dirac]}, \quad 0.008 \text{ [Majorana]}. \quad (19)$$

The x mean lifetime, dominated by $x \rightarrow \nu\nu\nu$ decays, can range between about 50 s (at the limit where $|U_{\mu x}| \gg |U_{\tau x}|$) to about 5×10^{-3} s (where $|U_{\tau x}|$ approaches its upper limit from Eq.(19)). Thus the x mean decay length is always much greater than the distance to the KARMEN detector, as required. Also at the lower end of this lifetime range, the cosmological and astrophysical constraints may perhaps be evaded.

We now address the further implications of the x -neutrino scenario for laboratory experiments. This scenario implies that, with the stopped π^+ decay chain as the neutrino source, x will be produced not only via $\pi^+ \rightarrow \mu^+x$ (giving the time-signatured anomaly in the KARMEN detector), but also via $\pi \rightarrow e^+x$ and $\mu^+ \rightarrow \bar{\nu}_\mu x e^+, \bar{x}\nu_e e^+$ channels. It is interesting to ask how many of these x should decay in the KARMEN detector (or other detectors), compared to the anomaly events, and what their signatures may be.

(a) The $\pi^+ \rightarrow e^+x$ channel. The rate depends on $|U_{ex}|^2$. The fraction that decay in a given detector depends inversely on the momentum with which x is produced. Hence the ratio of detected x decays from this channel compared to ‘‘anomaly’’ events from $\pi^+ \rightarrow \mu^+x$ is

$$\frac{N(\pi \rightarrow ex : x \text{ detected})}{N(\pi \rightarrow \mu x : x \text{ detected})} = \frac{|U_{ex}|^2 [m_\pi^2 (m_e^2 + m_x^2) - (m_e^2 - m_x^2)^2]}{|U_{\mu x}|^2 [m_\pi^2 (m_\mu^2 + m_x^2) - (m_\mu^2 - m_x^2)^2]} \simeq 0.15 \frac{|U_{ex}|^2}{|U_{\mu x}|^2} \quad (20)$$

In these events x has velocity $\beta_x = 0.89$ and reaches the detector essentially in coincidence with the prompt ν_μ burst from the initial pion pulse, well within the resolution defined by the 100 ns pulse length at the KARMEN source. For solutions with dominant $x \rightarrow e^-e^+\nu$ visible decays, the spectrum of visible energy (summed e^+e^- kinetic energies) is shown in Fig.2, including initial x polarization and folding in the relative decay probability in a detector. About 76% of such detected decays have visible energy greater than 40 MeV, whereas each prompt ν_μ carries only 29.8 MeV total energy, so these x -decay events should be quite distinctive. For the more restricted Majorana solutions, $|U_{ex}|^2/|U_{\mu x}|^2 \lesssim 10^{-2}$ and the $\pi \rightarrow ex$ signal is strongly suppressed. Solutions with dominant $x \rightarrow \nu\gamma$ visible decays necessarily have $|U_{ex}|^2 \ll |U_{\mu x}|^2 + |U_{\tau x}|^2$; if this is achieved with $|U_{\mu x}|^2 < |U_{ex}|^2 \ll |U_{\tau x}|^2$, then the $\pi \rightarrow ex$ production channel will be important, giving decay photon energies from 4 to 70 MeV with mean energy 26 MeV, to be compared with a narrow spike at $E_\gamma = 17$ MeV from anomaly events.

(b) The $\mu^+ \rightarrow \bar{\nu}_\mu x e^+$ channel. Once again the rate depends on $|U_{ex}|^2$ and the fraction decaying in a given detector depends inversely on the x -momentum. Numerical calculations give the detected event ratio:

$$\frac{N(\pi^+ \rightarrow \mu^+ \rightarrow \bar{\nu}_\mu e^+ x : x \text{ detected})}{N(\pi \rightarrow \mu x : x \text{ detected})} \simeq 0.38 \frac{|U_{ex}|^2}{|U_{\mu x}|^2}. \quad (21)$$

There is a spread of velocities $0 < \beta_x < 0.95$, but these events are smeared anyway by the parent muon lifetime and arrive with essentially the same time distribution as the $\bar{\nu}_\mu$ and ν_e interaction events. The detected visible energy spectrum for solutions with dominant $x \rightarrow e^-e^+\nu$, calculated for the $\mu \rightarrow x \rightarrow ee\nu$ cascade with full spin-correlated decay matrix elements [34], is shown in Fig.2; it has mean value $\langle T_{\text{vis}} \rangle \simeq 26$ MeV. This spectrum roughly resembles the $^{12}\text{C}(\nu_e, e^-)X$ spectrum shown in Ref. [1], but has a longer tail above 35 MeV, so it should be possible to distinguish one from the other. As with channel (a) above, this channel is suppressed by $|U_{ex}|^2/|U_{\mu x}|^2 \lesssim 10^{-2}$ for Majorana $x \rightarrow e^-e^+\nu$ solutions, but is important for a subset of $x \rightarrow \nu\gamma$ solutions, for which the decay photon energies extend from 5 to 53 MeV with mean value 26 MeV.

(c) The $\mu^+ \rightarrow \bar{x}\nu_e e^+$ channel. Here the rate depends on $|U_{\mu x}|^2$ instead, like the ‘‘anomaly’’ channel $\pi \rightarrow \mu x$. Numerical calculations give the detected event ratio:

$$\frac{N(\pi^+ \rightarrow \mu^+ \rightarrow \bar{x}\nu_e e^+ x : \bar{x} \text{ detected})}{N(\pi \rightarrow \mu x : x \text{ detected})} \simeq 0.40. \quad (22)$$

As with channel (b), these events have essentially the same time distribution as the $\bar{\nu}_\mu$

and ν_e interaction events; on the other hand, the number of these events compared to time-anomaly events is now firmly predicted. The detected visible energy spectrum for $x \rightarrow e^-e^+\nu$ solutions is shown in Fig.2; like case (b) it has mean value $\langle T_{\text{vis}} \rangle \simeq 26$ MeV and can be distinguished from conventional $^{12}\text{C}(\nu_e, e^-)X$ by the tail above 35 MeV. For $x \rightarrow \nu\gamma$ solutions, the decay photon again has energies between 5 and 53 MeV with mean value 28 MeV.

To summarize, a mainly-sterile neutrino interpretation for x is consistent with all laboratory constraints, within limited ranges of mixing parameters, for both Dirac and Majorana options, although there are some astrophysical and cosmological problems. Solutions with dominant $x \rightarrow e^-e^+\nu$ visible decays are constrained by Eqs.(6)-(13),(17); here the mixing parameters $|U_{\mu x}|$ and $|U_{ex}|$ are adjusted to give compatible values of branching fraction B and visible-mode lifetime τ in Fig.1 (while $|U_{\tau x}|$ is negligible). Alternative solutions with dominant $x \rightarrow \nu\gamma$ visible decays are constrained by Eqs.(6),(16),(18)-(19); here B and τ are determined by $|U_{\mu x}|$ and $|U_{\tau x}|$ instead (while $|U_{ex}|$ is negligible). Such interpretations imply that other sources of x -production should contribute appreciable additional x -decay events in the KARMEN detector, with different time-structures; in channels (a) and (b) the event rate depends on $|U_{ex}|$ and is appreciable in some Dirac $x \rightarrow e^-e^+\nu$ solutions and some $x \rightarrow \nu\gamma$ solutions, but in channel (c) the event rate is always 40% of the anomaly event rate. Similar x -decay signals should also appear in the LSND detector [2]. Since both detectors have approximately the same density, and since both ν -interaction and x -decay events have the same inverse-square dependence on distance L (so long as $L \ll \beta_x \gamma_x \tau_x c$), the ratio of interactions to decays should be approximately the same in both experiments. Such x decays could conceivably provide a background to the $\bar{\nu}_\mu \rightarrow \bar{\nu}_e$ oscillation search currently under way [3], although the $\bar{\nu}_e p \rightarrow e^+ n$ signal is distinguishable in principle by detecting the delayed 2.2 MeV gamma from the subsequent neutron capture $n(p, d)\gamma$. In high-energy neutrino beams, however, where the parent pions have been boosted to energies $E_\pi = \gamma m_\pi$ with $\gamma \gg 1$, the number of x -decays in a given detector volume will scale down as $p_x^*/[E_x^* \gamma]$ (where p^* and E^* are π -restframe momentum and energy) while the ν interactions will scale up as γ ; thus the fraction that are decays decreases as $1/\gamma^2$ and rapidly becomes negligible. Hence $x \rightarrow e^+e^-\nu$ decays cannot contribute significantly to the apparent e/μ excess in atmospheric neutrino events [35], where the parent pions and kaons have energies of

$\mathcal{O}(\text{GeV})$. Similarly, there should be a negligible $x \rightarrow e^+e^-\nu$ contribution in accelerator experiments such as BNL-E776 [36] which set an upper limit on $\nu_\mu \rightarrow \nu_e$ and $\bar{\nu}_\mu \rightarrow \bar{\nu}_e$ oscillations using GeV neutrinos.

Finally, we note that isosinglet (sterile) neutrinos occur naturally in $SO(10)$ and E_6 GUT models, as members of the basic fermion families [19]. A very light ($\approx 10^{-2}$ eV) sterile neutrino has been suggested as a possible [37] or even necessary [38] participant in solar neutrino oscillations, while one with a mass of $\mathcal{O}(\text{keV})$ is a good candidate for ‘warm’ dark matter [39]. Heavy singlet neutrinos could cause distinctive lepton-number-nonconserving, lepton-flavour-changing and lepton-universality-breaking effects in a wide range of laboratory processes [40].

Acknowledgments

RJNP thanks J. Kleinfeller, I. Blair and J. Guy for conversations; VB thanks R. Imlay for a discussion; SS thanks N. Booth, R. Mohapatra and G. Raffelt for helpful comments. This research was supported in part by the U.S. Department of Energy under Grant No. DE-FG02-95ER40896 and in part by the University of Wisconsin Research Committee with funds granted by the Wisconsin Alumni Research Foundation. SS is a PPARC Advanced Fellow and acknowledges support from the EC Theoretical Astroparticle Network.

References

- [1] KARMEN collaboration: B. Armbruster *et al*, Phys. Lett. **B348** (1995) 19.
- [2] R.A. Reeder *et al*, Nucl. Instr. and Meth. **A334** (1993) 353.
- [3] D.O. Caldwell, in *Trends in Astroparticle Physics*, Stockholm 1994, eds. L. Bergström *et al*, Nucl. Phys. **B**, Proc. Suppl. (in press).
- [4] A. De Rujula and S.L. Glashow, Phys. Rev. Lett. **45** (1980) 942;
P.B. Pal and L. Wolfenstein, Phys. Rev. **D25** (1982) 766;
M. Gronau and R. Yahalom, Phys. Rev. **D30** (1984) 2422.
- [5] A. Hime, R.J.N. Phillips, G.G. Ross and S. Sarkar, Phys. Lett. **B260** (1991) 381.

- [6] Particle Data Group, Phys. Rev. **D50** (1994) 1173.
- [7] R.E. Shrock, Phys. Rev. **D24** (1981) 1232, 1275 .
- [8] CHARM collaboration: F. Bergsma *et al*, Phys. Lett. **128B** (1983) 361.
- [9] BEBC-WA66 collaboration: A.M. Cooper-Sarkar *et al*, Phys. Lett. **160B** (1985) 207.
- [10] PS-191 collaboration: G. Bernardi *et al*, Phys. Lett. **166B** (1986) 479.
- [11] N. De Leener-Rosier *et al*, Phys. Rev. **D43** (1991) 3611;
T. Numao *et al*, *Proc. Beyond the Standard Model III*, Ottawa, eds. S. Godfrey and P. Kalyniak (World Scientific, Singapore, 1993);
G. Czapek *et al*, Phys. Rev. Lett. **70** (1993) 17;
D.I. Britton *et al*, Phys. Rev. **D49** (1994) 28.
- [12] T. Bernatowicz *et al*, Phys. Rev. Lett. **69** (1992) 2341;
A. Balysh *et al*, Phys. Lett. **B283** (1992) 32, preprint hep-ex/9502007;
J.-C. Vuilleumier *et al*, Phys. Rev. **D48** (1993) 1009.
- [13] P. Bamert, C.P. Burgess and R.N. Mohapatra, Nucl Phys. **B438** (1995) 3.
- [14] S. Petcov, Sov. J. Nucl. Phys. 25 (1977) 344, (Erratum) 25 (1978) 698;
B.W. Lee, S. Pakvasa, H. Sugawara and R.E. Shrock, Phys. Rev. Lett. **38** (1977) 937;
T.-P. Cheng and L.-F. Li, Phys. Rev. **D16** (1977) 1425;
W.J. Marciano and A. Sanda, Phys. Lett. **67B** (1977) 303.
- [15] ARGUS collaboration: H. Albrecht *et al*, Phys. Lett. **B292** (1992) 221.
- [16] CLEO II collaboration: D. Cinabro *et al*, Phys. Rev. Lett. **70** (1993) 3700.
- [17] ALEPH collaboration: D. Buskulic *et al*, preprint CERN PPE/95-003.
- [18] The LEP Collaborations: preprint CERN PPE/94-187.
- [19] G.B. Gelmini and E. Roulet, preprint UCLA/94/TEP/36 [hep-ph/9412278];
R.N. Mohapatra and P.B. Pal, *Massive Neutrinos in Physics and Astrophysics* (World Scientific, 1991).

- [20] D.A. Dicus, E.W. Kolb and V.L. Teplitz, *Astrophys. J.* **221** (1978) 327;
E.W. Kolb and T. Goldman, *Phys. Rev. Lett.* **43** (1979) 897.
- [21] S. Sarkar and A.M. Cooper, *Phys. Lett.* **148B** (1984) 347.
- [22] D. Lindley, *Astrophys. J.* **294** (1985) 1.
- [23] S. Sarkar, *Proc. XVII Int. Symp. on Multiparticle Dynamics*, Seewinkel, eds. M. Markytan *et al*(World Scientific, 1986) p 863;
L.M. Krauss, *Proc. Telemark Minconference on Neutrino Masses* (1985).
- [24] E.W. Kolb and R.J. Scherrer, *Phys. Rev.* **D25** (1982) 1481;
N. Terasawa, M. Kawasaki and K. Sato, *Nucl. Phys.* **302** (1988) 697;
S. Dodelson, G. Guyk and M.S. Turner, *Phys. Rev.* **D49** (1994) 5068.
- [25] A. Dar and S. Dado, *Phys. Rev. Lett.* **59** (1987) 2368;
L. Oberauer, C. Hagner, G. Raffelt and E. Rieger, *Astropart. Phys.* **1** (1993) 377;
R.N. Mohapatra, S. Nussinov and X. Zhang, *Phys. Rev.* **D49** (1994) 3434.
- [26] S.W. Falk and D.N. Schramm, *Phys. Lett.* **B79** (1978) 511;
R. Cowsik, D.N. Schramm and P. Höflich, *Phys. Lett.* **B218** (1989) 91.
- [27] G. Sigl and M.S. Turner, *Phys. Rev.* **D51** (1995) 1499.
- [28] G. Raffelt and G. Sigl, *Astpart. Phys.* **1** (1993) 165;
X. Shi and G. Sigl, *Phys. Lett.* B323 (1994) 360.
- [29] K. Kainulainen, J. Maalampi and J.T. Peltoniemi, *Nucl. Phys.* **B358** (1991) 435;
B. Mukhopadhyaya and R. Gandhi, *Phys. Rev.* **D46** (1992) 3682.
- [30] G. Raffelt, private communication.
- [31] A. Manohar, *Phys. Lett.* **B186** (1987) 370;
R. Barbieri and A. Dolgov, *Nucl. Phys.* **B349** (1991) 743;
K. Enqvist, K. Kainulainen and M. Thompson, *Nucl. Phys.* **B373** (1992) 498;
X. Shi, D.N. Schramm and B.D. Fields, *Phys. Rev.* **D48** (1993) 2563.
- [32] P. Langacker, B. Sathiapalan and G. Steigman, *Nucl. Phys.* **B266** (1986) 669.

- [33] BEBC-WA66 collaboration: A.M. Cooper-Sarkar, private communication (quoted by K.S. Babu *et al*, Phys. Lett. **B321** (1994) 140).
- [34] V. Barger, J. Ohnemus and R.J.N. Phillips, Phys. Rev. **D35** (1987) 166.
- [35] K.S. Hirata *et al*, Phys. Lett. **B280** (1992) 146;
Y. Fukuda *et al*, Phys. Lett. **B335** (1994) 237.
- [36] L. Borodovsky *et al*, Phys. Rev. Lett. **68** (1992) 274.
- [37] V. Barger *et al*, Phys. Rev. **D43** (1991) 1759;
C.-S. Lim and W.J. Marciano, Phys. Rev. **D37** (1988) 1368.
- [38] G.M. Fuller, J. Primack and Y.-Z. Qian, preprint DOE-ER-40561-185 [astro-ph/9502081].
- [39] S. Dodelson and L.M. Widrow, Phys. Rev. Lett. **72** (1994) 17.
- [40] see P. Langacker, L. Luo and A.K. Mann, Rev. Mod. Phys. **64** (1992) 87;
J. Bernabeu *et al*, Phys. Rev. Lett. **71** (1993) 2695;
A. Ilakovac and A. Pilaftsis, Nucl. Phys. **B437** (1995) 491;
P. Roy, preprint TIFR-TH-94-35 [hep-ph/9501209]; and references therein.

Figures

1. Correlation between the x mean lifetime and production branching ratio $B = \Gamma(\pi \rightarrow \mu x)/\Gamma(\pi \rightarrow \mu\nu)$, needed to explain the KARMEN anomaly; the solid curve is taken from Ref. [1] and the dashed curve is its extrapolation. The $|U_{\mu x}|^2$ scale is derived from Eq.(4) for B . The $|U_{ex}|^2$ scale is derived from Eq.(5) for the case of dominant $x \rightarrow e^-e^+\nu$ visible decays with Dirac x . The most stringent laboratory constraints on the $|U_{\alpha x}|$ values are also shown [6,7,10,11]. For Majorana x there is an additional constraint $|U_{ex}|^2 \lesssim 6 \times 10^{-8}$ and the $|U_{ex}|^2$ scale moves left by a factor of 2.
2. Visible energy spectra for $x \rightarrow ee\nu$ decays from various sources, weighted by the inverse of the x momentum for the relative decay probability in a given detector.

The solid curve denotes the stopped $\pi^+ \rightarrow \mu^+ x$ source; dotted, dashed, and dot-dashed curves denote the $\pi^+ \rightarrow e^+ x$, $\pi^+ \rightarrow \mu^+ \rightarrow \bar{\nu}_\mu x e^+$ and $\pi^+ \rightarrow \mu^+ \rightarrow \bar{x} \nu_e e^+$ sources, respectively.

Erratum

In the case that neutrino x is mainly isosinglet (sterile), we overlooked neutral-current contributions to the decay $x \rightarrow \nu e^+ e^-$, as pointed out by J. Peltoniemi (hep-ph/9606228). The corrected width for small mixing is

$$\Gamma(x \rightarrow \nu e^+ e^-) = 390K \left[(1 + 4x_W + 8x_W^2)|U_{ex}|^2 + (1 - 4x_W + 8x_W^2)(|U_{\mu x}|^2 + |U_{\tau x}|^2) \right] \text{ s}^{-1},$$

where $x_W \equiv \sin^2 \theta_W = 0.23$, $K = 1(2)$ for Dirac (Majorana) x and the $|U_{ex}|^2$ term includes charged-current contributions. The visible decay width (including $x \rightarrow \nu \gamma$) and total width then become

$$\begin{aligned} \Gamma_{\text{vis}} &= K [920|U_{ex}|^2 + 210|U_{\mu x}|^2 + 210|U_{\tau x}|^2] \text{ s}^{-1}, \\ \Gamma_{\text{tot}} &= K [2470|U_{ex}|^2 + 1760|U_{\mu x}|^2 + 1760|U_{\tau x}|^2] \text{ s}^{-1}. \end{aligned}$$

The KARMEN event rate determines the product B ($\pi^+ \rightarrow \mu^+ x$) $\Gamma_{\text{vis}} \simeq 3 \times 10^{-11} \text{ s}^{-1}$ with $B = 0.0285 |U_{\mu x}|^2$ as before, which allows different types of solution:

(A) If $|U_{ex}|^2$ dominates Γ_{vis} , we obtain $|U_{ex}U_{\mu x}|^2 \simeq 1.1K^{-1} \times 10^{-12}$. For Majorana x , no such solutions are compatible both with the constraint Eq.(9) and with $|U_{ex}|^2$ dominance of Γ_{vis} . For Dirac x there are acceptable solutions near $|U_{ex}|^2 \sim |U_{\mu x}|^2 \sim 10^{-6}$; but as $|U_{ex}|$ decreases, $|U_{\mu x}|$ increases and they merge into category (B).

(B) If $|U_{\mu x}|^2$ dominates Γ_{vis} , we obtain a fixed value $|U_{\mu x}|^2 \simeq 2.3K^{-1/2} \times 10^{-6}$. These solutions allow ranges of $|U_{ex}|, |U_{\tau x}| < |U_{\mu x}|$, but when $|U_{\tau x}|$ increases further they merge into category (C).

(C) If $|U_{\tau x}|^2$ dominates Γ_{vis} , we obtain $|U_{\mu x}U_{\tau x}|^2 \simeq 5K^{-1} \times 10^{-12}$, with $1.5K^{-1} \times 10^{-6} < |U_{\tau x}|^2 < 1$, where the upper (unitarity) limit cannot be approached closely because x cannot be the main component of ν_τ . Solutions (A) and (B) give mean lifetimes $\tau_x \sim (150 - 300) \text{ s}$, but (C) covers the range $\tau_x \sim (0.001 - 150) \text{ s}$.

The neutral-current contributions now guarantee that $x \rightarrow \nu e^+ e^-$ is always the dominant visible mode. Eqs.(16)-(17) are invalidated and some parameters change, but our qualitative conclusions about the existence of solutions (especially short-lived type-(C) cases) remain broadly unchanged.

Concerning additional sources of x at KARMEN, the $\pi^+ \rightarrow ex$ and $\mu^+ \rightarrow \bar{\nu}_\mu x e^+$ channels depend on the ratio $|U_{ex}/U_{\mu x}|^2$ as before; this ratio is $\lesssim 1$ for (A) and (B) but can be large for type-(C) solutions. The $\mu^+ \rightarrow \bar{x} \nu_e e^+$ rate is fixed and unchanged.

This figure "fig1-1.png" is available in "png" format from:

<http://arxiv.org/ps/hep-ph/9503295v4>

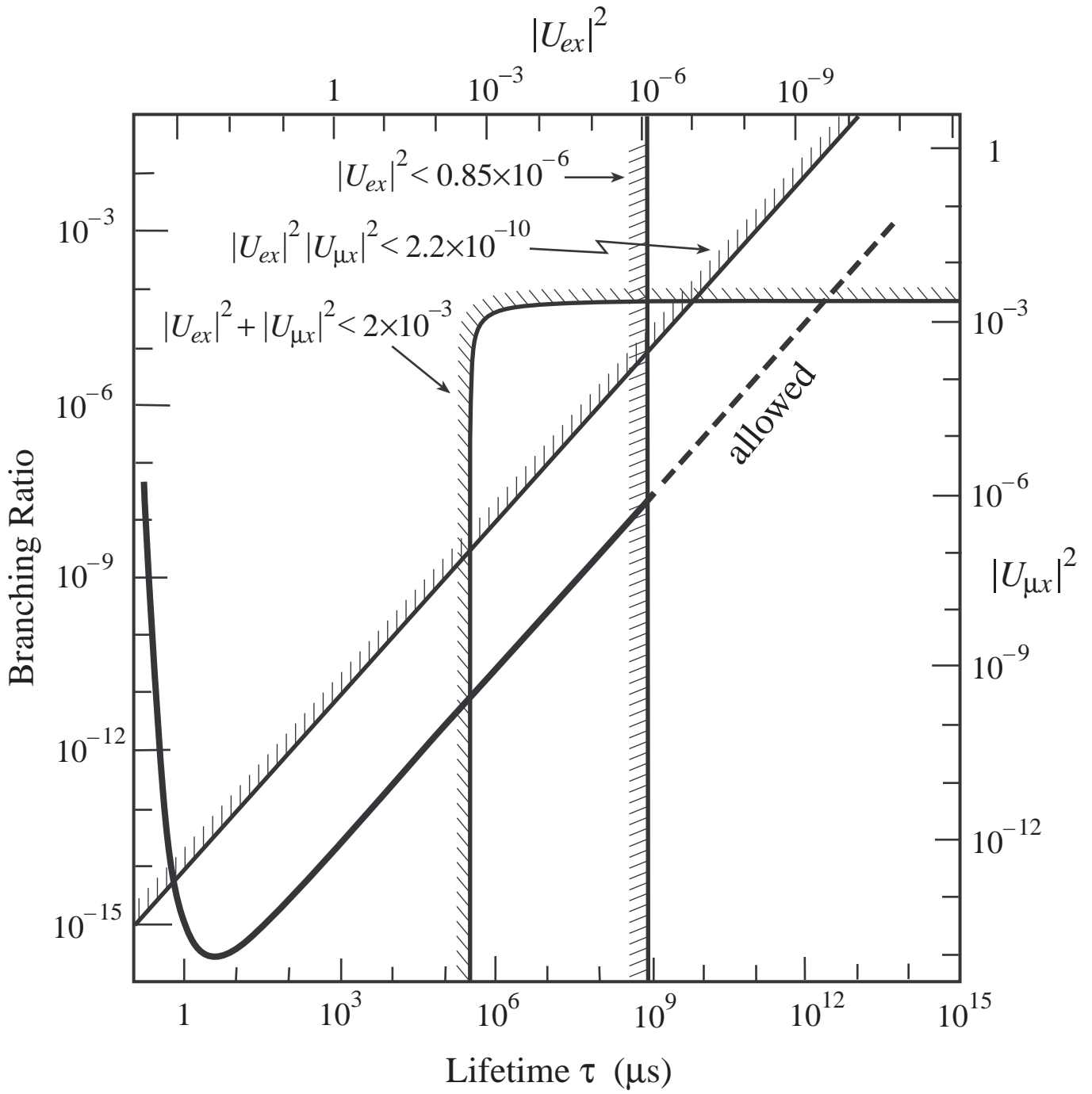


Figure 1

This figure "fig1-2.png" is available in "png" format from:

<http://arxiv.org/ps/hep-ph/9503295v4>

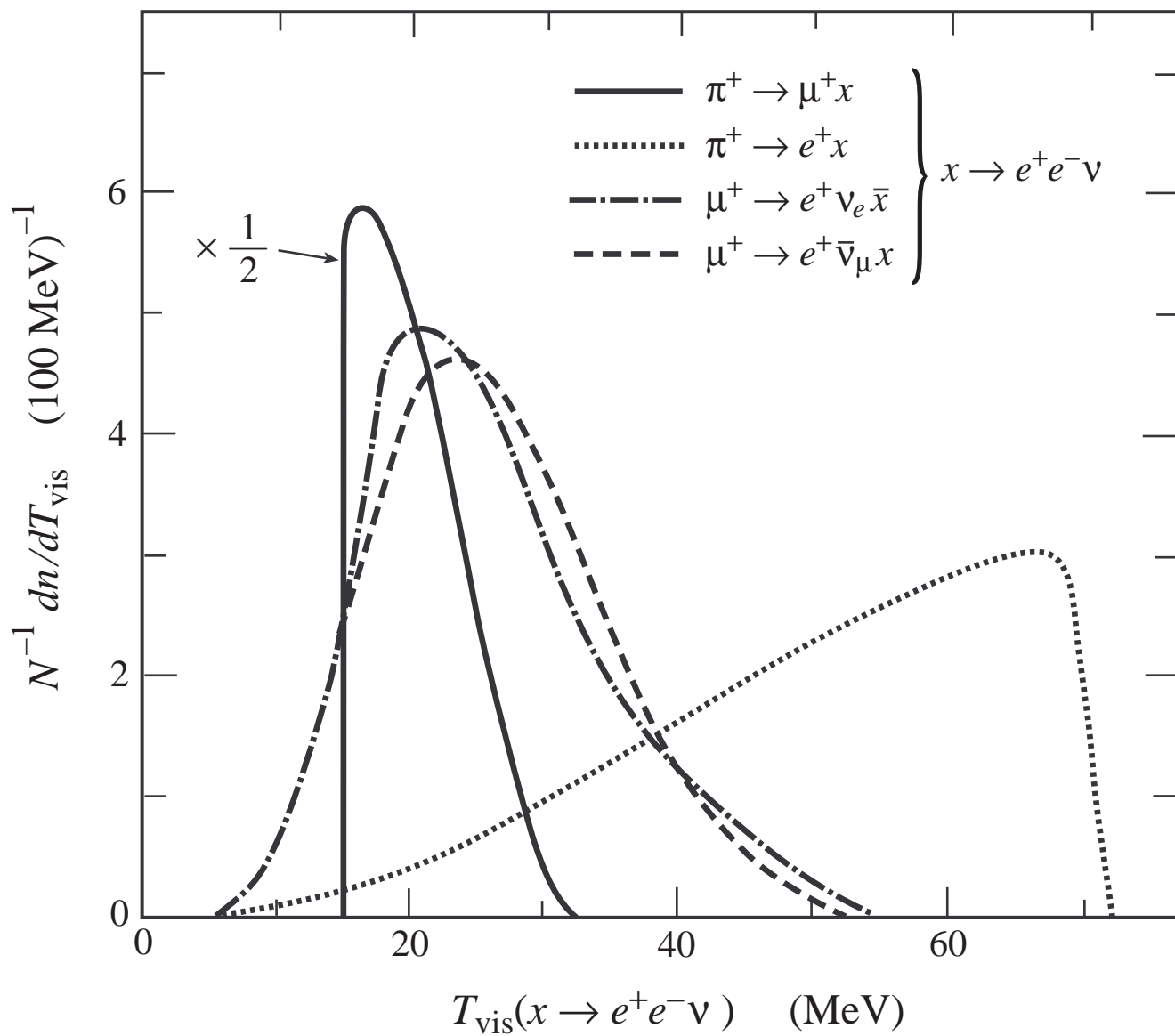


Figure 2